International Journal of Nanomedicine

Dovepress
open access to scientific and medical research

Open Access Full Text Article

ORIGINAL RESEARCH

Enhanced photo/chemo combination efficiency against bladder tumor by encapsulation of DOX and ZnPC into in situ-formed thermosensitive polymer hydrogel

This article was published in the following Dove Press journal:
International Journal of Nanomedicine

Zhongming Huang
He Xiao
Xiangyun Lu
Weigang Yan
Zhigang Ji

Department of Urology, Peking Union Medical College Hospital, Chinese Academy of Medical Sciences and Peking Union Medical College, Beijing 100730, China

Background: Chemotherapy after transurethral resection is commonly recommended for bladder cancer. However, studies have shown that chemotherapy solely can hardly decrease progression rates of bladder cancer. The combination of chemotherapeutic agents with photodynamic therapy (PDT), a new promising localized therapy, may become a workable strategy for combating bladder cancer. This study reports the combination of doxorubicin (DOX)-based chemotherapy and zinc phthalocyanine (ZnPC)-based PDT using in situ-formed thermal-responsive copolymer hydrogel.

Materials and methods: The copolymer was synthesized by polymerization of 3-caprolactone, 1,4,8-trioxa[4.6]spiro-9-undecanone and poly(ethylene glycol) and was abbreviated as PCL-PTSUO-PEG. The thermal-responsive nanoparticles (TNPs) were prepared by the nanoprecipitation technology. The thermal-responsive hydrogel was formed after 37°C heating of TNP solution. The size, morphology and dynamic viscosity of hydrogel were detected. The in vitro drug release profile of TNP/DOX/ZnPC was performed. Cell uptake, cell inhibition and ROS generation of TNP/DOX/ZnPC were studied in 5637 cells. The in vivo antitumor activity of TNP/DOX/ZnPC was evaluated in nude mice bearing 5637 cells xenograft.

Results: TNP/DOX and TNP/ZnPC had an average diameter of 102 and 108 nm, respectively. After being heated at 37°C for 5 minutes, TNP/DOX and TNP/ZnPC solution turned uniform light red and dark green hydrogel. ZnPC encapsulation designed by TNP could significantly improve its aqueous solubility to 1.9 mg/mL. Cell inhibition showed that the best cell inhibition was found, with cell viability of 18.5%, when the weight ratio of DOX and ZnPC encapsulated in the TNP reached about 1:5. TNP/DOX/ZnPC generated relative high level of ROS with 4.8-fold of free ZnPC and 1.6-fold of TNP/ZnPC. TNP/DOX/ZnPC showed only 8-fold of relative tumor growth without obvious toxicity to the mice.

Conclusion: Thermosensitive thermal-responsive hydrogel reported in this contribution are promising in situ-formed matrix for DOX- and ZnPC-based photo/chemo combination treatment for bladder cancer therapy.

Keywords: chemotherapy, photodynamic therapy, combination therapy, hydrogel, thermosensitive, bladder cancer

Correspondence: Zhigang Ji
Department of Urology, Peking Union Medical College Hospital, Chinese Academy of Medical Sciences and Peking Union Medical College, No 1 Shuaifuyuan Wangfujing, Dongcheng, Beijing 100730, China
Tel +86 106 915 2511
Fax +86 106 915 2511
Email zhigangji@163.com

Introduction

Bladder cancer is a complex disease associated with high morbidity and mortality rates if not treated optimally.[1,2] Clinically, chemotherapy after transurethral resection is commonly recommended for bladder cancer. A meta-analysis of randomized

submit your manuscript | www.dovepress.com
Dovepress
http://dx.doi.org/10.2147/IJN.S179226

trials showed that patients with intermediate-risk nonmuscle invasive bladder cancer benefit from 1-year maintenance of intravesical chemotherapy after transurethral resection.[3] However, no studies have shown that chemotherapy solely decreases progression rates of intermediate-risk nonmuscle invasive bladder cancer. In addition, reported 5-year cancer recurrence rates of nonmuscle invasive bladder range from 50% to 70%.[1]

Many traditional interventions, such as chemotherapy, radiotherapy and surgery, are employed for cancer treatment. However, with the side effects of current treatments such as low or moderate targetability, recurrence and evolution of drug-resistant over time, cancer is still a Gordian knot and life-threatening. Among the alternatives for cancer treatment currently being exploited, photodynamic therapy (PDT), initiated by the pioneering work of Dougherty et al,[4] has been attracting increasing attention over the last few decades due to its good selectivity, efficiency and minimal invasiveness. PDT is a localized therapy for diverse indications, including cancer, infectious diseases and cardiovascular disease.[5–7] Therefore, as a novel therapeutic technology, PDT, especially localized PDT, has promising potential for applying in bladder cancer treatment.

Photosensitizer (PS) is the key of PDT. Phthalocyanines (PCs) and their derivatives, after being unintended discovered in 1928, have since attracted much attention.[8] As the second generation of PSs, PCs show an extension of absorption spectrum, which offer the ability of greater tissue penetration.[9–11] Compared with the precursor porphyrin, the improved spectroscopic and photochemical properties of PCs increase its specificity for neoplastic targets.[12] In addition, the unique feature of central cavity endows the PCs, the capacity of accommodating 63 different elemental ions, which further increase its tissue penetration ability and intense absorption band in the red or near infrared region of electromagnetic spectrum. Among them, zinc phthalocyanine (ZnPC) is a highly potent PC derivative due to its attractive photophysical and photochemical properties.[13,14] However, the intermolecular forces of π–π conjugation of free-ZnPc lead to its low solubility and crystallization, making it unable to be directly applied on PDT therapy. ZnPC CGP55847, formulated in liposomes and developed by QLT Phototherapeutics (Vancouver, Canada), is the first PCs reaching PDT clinical trials (Phase I/II, Switzerland).[15] Therefore, drug delivery system for ZnPC is highly needed to extend its application in PDT.

The above challenges of PSs instigated the development of their incorporation within supramolecular platforms.[16,17] Supramolecular PS were initially designed as a means to alter its pharmacokinetics, and now the supramolecular formulation also further facilitates single agent–mediated deeper tissue photoactivation and extends new theranostic and phototherapy paradigms.[18–20] Nanoparticles that enhance PS delivery to tumors encompass the largest class of biomedical PS supramolecular formulations (nano-PS) explored thus far.[16,21,22] Liposomal verteporfin (Visudyne®), the only supramolecular porphyrin nanoparticle received Food and Drug Association approval for PDT in the treatment of choroidal neovasculature in age-related macular degeneration, pathological myopia and central serous chorioretinopathy, has also undergone investigation in some kinds of cancer PDT. However, it was plagued by low drug loading, inefficient drug release and opsonization by the immune system.[16] Despite improvements achieved in the delivery of PS to target tissue by active targeting and stimuli-responsive release from supramolecular platforms, many challenges still remain. The multifaceted and dynamic tumor microenvironment makes it difficult to find out precisely what kind of receptors were expressed and their expression level at any given time. However, systemically administered nano-PS may induce skin phototoxicity, which restricts dose escalation in PDT. In this regard, nanocarrier platforms with the topical delivery of PS may spare, if possible, the MPS sequestration and the healthy cells.

Some preclinical studies and clinical trials indicated that the combination of PDT with more traditional treatments such as specific chemotherapeutic agents may become a workable anticancer strategy.[23,24] On the premise that the overall efficacy is preserved or even augmented, photo/chemo combination therapy may allow the reduction of the dosage of individual drugs and consequently the lessening of important side effects. Mounting evidence suggested that this combination showed a prominent additive to synergistic effect over individual treatment when used alone. The study by Zakaria et al indicated that combination of ALA-PDT and Doxil® (nanodrug formulation of doxorubicin [DOX]) possessed a synergistic cytotoxic effect on MCF-7 (human breast adenocarcinoma cell line) cells through intrinsic and extrinsic apoptotic cell death induction.[25] Similarly, Diez et al demonstrated the efficacy of the combined therapy to overcome drug resistance in leukemic cell lines.[26] However, the combination protocols, including the time span, the sequence and the integration of individual treatment, are still far from being established. With advantages of co-loading, local administration and stimulus-responsive drug release, smart hydrogels may be useful in addressing drug combination regimen, thus achieving a positive outcome.[24]

Artzi et al developed an adhesive hydrogel patch that enabled the combination of local gene, drug and phototherapy and resulted in tumor regression and prevented recurrence in a colon cancer model.[27] Anjie et al developed thermosensitive micellar-hydrogel for enhanced in situ synergetic chemo/radio therapy with a single drug administration and reduced side effects.[28]

Inspired by the above works, especially the exciting improvements in hydrogel-based local combination therapy, we reasonably conceived a thermal-responsive hydrogel, which facilitates the topical delivery of PS and chemotherapeutic drugs simultaneously, may be a promising carrier to address the defects of systemically administered nanoplatforms in photo/chemo combination therapy. With reference to the work by Huang et al,[28] we developed an in situ-formed thermosensitive nanoparticle hydrogel of PCL-PTSUO-PEG (abbreviated as TNP^{GEL}) that can coencapsulate ZnPC and DOX for effective inhibition of bladder 5637 cells. This work further studies the feasibility of using TNP^{GEL} as an effective carrier for ablation of bladder tumor in mice model.

Materials and methods

Materials

Doxorubicin hydrochloride (98%) was purchased from Wuhan Hezhong Biochem Co., Ltd. (Wuhan, China); 5637 cells were maintained in our laboratory. RPMI 1640 Medium, DAPI, MTT and other chemicals were provided by Sigma-Aldrich (St Louis, MO, USA). Reactive Oxygen Species Assay Kit was purchased from Shanghai Yisheng Biotech Co., Ltd. (Shanghai, China). 5637 cells was bought from ATCC (ATCC® HTB-9™). Nude female BALB/c mice of 4–6 weeks old were acquired from Vital River Laboratory Animal Technology Co., Ltd. (Beijing, China). All animal experiments in our study were performed in accordance with the guidelines of the Administration of Experimental Animals (Beijing, revised Dec. 2004) and approved by the Animal Ethics Committee of Peking Union Medical College Hospital.

Preparation and characterization of copolymer and drug-loaded TNPs

The copolymer was synthesized and drug-loaded TNPs were prepared based on methods reported in references.[28,29] The copolymer was characterized by hydrogen nuclear magnetic resonance (^{1}H NMR) (Bruker ARX 300). For DOX-loaded TNPs (TNP/DOX), a mixture of DOX (5 mg) and PCL-PTSUO-PEG copolymer (500 mg) were dissolved in 5 mL DMSO, then the mixture solution was added dropwise into 10 mL PBS buffer under stirring and then the mixture was stirred at room temperature for 12 hours. Then the DMSO of the system was evaporated. The DOX-encapsulated nanoparticles solution was then centrifuged at 8,000 rpm for 5 minutes to remove the unencapsulated DOX. The supernatant was collected and powder of TNP/DOX was obtained after lyophilization. The ZnPC-loaded TNPs (TNP/ZnPC) was prepared with same method with the addition of ZnPC. The size of TNPs was measured by DLS. Drug-loading content (DLC) and drug-loading efficiency (DLE) were quantified by UV-vis spectrophotometer.

Preparation of thermosensitive hydrogels

The TNP/drug solution was prepared by redispersion of above-prepared TNP/drug powder in PBS at room temperature. TNP/DOX/ZnPC solution was prepared by the mixture of TNP/DOX and TNP/ZnPC at designate mass ratio. Blank TNP^{GEL} or drug-loaded TNP hydrogel was formed by 37°C heating of blank TNP solution (in PBS) or drug-loaded nanoparticle solution (in PBS) at the polymer concentration of 20% (W/W) for 5 minutes. The gelation property was studied using vial inversion, and rheology test was performed on an AR 2000ex (TA instrument) system using 40 mm parallel plates at the gap of 500 μm. The viscosity analysis of TNP solution with temperature at the polymer concentration of 20% (W/W) was performed with heating rate of 0.5°C/min at the strain of 2% and frequency of 2 rad/seconds. The modulus analysis of TNP^{GEL} with frequency sweep was performed at the strain of 2%. The micromorphology of the TNP^{GEL} was observed by scanning electron microscope (SEM).

In vitro drug release

Drug release studies were performed using dialysis method and quantitatively studied using UV spectrophotometer. TNP/DOX and TNP/ZnPC were prepared as described above. TNP/DOX/ZnPC solution in PBS buffer (pH 7.4) at a concentration of 20% (W/W) was prepared by the mixture of TNP/DOX and TNP/ZnPC with a weight ratio of DOX and ZnPC, 1:5. About 1 mL of TNP/DOX/ZnPC solution was added to a dialysis bag (molecular weight cutoff, 1 kDa) and dialyzed against 10 mL PBS buffer at 37°C for 35 days. One milliliter of dialysate was taken out for quantitative research at each time point, at the same time, another 1 mL of fresh PBS buffer was added into the dialysate buffer.

Cellular uptake experiment

5637 cells were seeded on confocal microscopic dish at a density of 1×10^5 per dish and incubated for 24 hours. A certain amount of free DOX or free ZnPC and TNP/DOX/ZnPC

solution was added after removing original medium, and the drug concentrations of DOX and ZnPC were maintained at 17.8 and 20 μg/mL, respectively. After being incubated for 4 hours, the cells were washed three times with cold PBS and fixed with 4% paraformaldehyde solution for 20 minutes. After being stained with 500 μL DAPI for 10 minutes, cells were examined using inverted fluorescence microscopy.

In vitro cell killing efficiency

In vitro cell killing efficiency of drug-loaded TNPs and their combinations were evaluated by MTT assay. 5637 cells were seeded into 96-well plates at a density of 5,000 cells per well. After 24 hours of incubation, cells were treated with TNP/DOX at TNP/ZnPC at different drug weight ratios. After 4 hours of incubation, the cells were exposed to laser of 660 nm for 90 seconds with an intensity of 100 J/cm^2 (Photon Lase I; DMC, São Carlos, São Paulo, Brazil). After light exposure, the cell culture was further incubated for 24 hours at 37°C. Finally, MTT assay was performed to evaluate the relative cell viability.

Intracellular ROS generation

Intracellular ROS generation was evaluated by 2′,7′-dichlorodihydrofluorescein-diacetate (DCFH-DA). 5637 cells were seeded into 96-well plates at a density of 5,000 cells per well. After 24 hours of incubation, cells were treated with DOX, ZnPC, TNP/ZnPC and TNP/DOX/ZnPC at DOX/ZnPC weight ratio of 1:5 (DOX and ZnPC concentrations were 2 and 10 μg/mL, respectively). After 4 hours of incubation, the cells were exposed to laser of 660 nm for 90 seconds with an intensity of 100 J/cm^2 or not. Finally, 100 μL of DCFH-DA solution (10 μM) was added, and the mixture was incubated at 37°C for additional 20 minutes. The cells were then washed twice with PBS, and the fluorescence intensity was measured by a Varioskan Flash with excitation and emission wavelengths of 485 and 525 nm, respectively.

In vivo antitumor activity

The in vivo antitumor activity of TNP/DOX/ZnPC was evaluated in nude mice-bearing 5637 cells xenograft. When tumor volume reached ~100 mm^3, mice were randomly grouped into four groups of PBS, TNP/DOX, TNP/ZnPC and TNP/DOX/ZnPC. TNP/DOX and TNP/ZnPC were mixed with DOX/ZnPC weight ratio of 1:5 for TNP/DOX/ZnPC treatment. DOX and/or ZnPC was administrated at a total dose of 20 mg/kg body weight once per mouse via peritumoral administration with an injection volume of 200 μL. Tumor volumes were measured using a caliper at designated times and calculated according to the formula, tumor volume = $a^2 \times b/2$, where

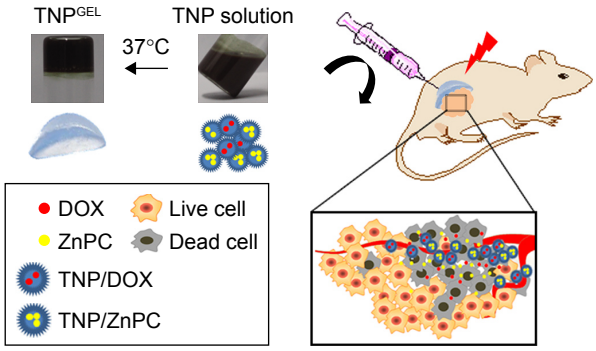

Figure 1 The schematic illustration of photo/chemo combination therapy via in situ-formed thermal-sensitive polymer hydrogel (TNP^{GEL}) in a xenograft tumor model.
Abbreviations: DOX, doxorubicin; TNP, thermal-responsive nanoparticle; TNP/DOX, TNP encapsulated with DOX; TNP^{GEL}, Hydrogel formed by 37°C heating in vitro or formed peritumor in nude mice; TNP/ZnPC, TNP encapsulated with ZnPC; ZnPC, zinc phthalocyanine.

a is the shorter diameter and b is the longer one. Body weight of each animal was also recorded every 2 days.

Statistical analysis

All data are presented as mean ± SDs. The differences among groups were determined using Student's t-test (GraphPad Prism 6.0) and $P<0.05$ was considered to be statistically significant.

Results and discussion

Characterization of copolymer and drug encapsulation

^{1}H NMR showed the successful synthesis of the tri-block copolymer PCL-PTSUO-PEG (Figures S1 and S2). As shown schematically in Figure 1, DOX and ZnPC were loaded into the TNP during the self-assembly of amphiphilic PCL-PTSUO-PEG (TNPs). Because DOX and ZnPC was loaded into TNPs separately and then purified lyophilized powder of TNP/DOX and TNP/ZnPC could be mixed with designate ratios to obtain specific composite hydrogels (named TNP/DOX/ZnPC^{GEL}) for chemo/photo combination therapy. The encapsulation of DOX and ZnPC was determined indirectly by UV spectrophotometer analysis of the unloaded drug. When the feeding weight of DOX or ZnPC was 1 mg per 100 mg TNPs, the drug-loading process yields the DLE of 85.3%±2.1% and 95.2%±1.5% for DOX and ZnPC, with corresponding DLC was 0.84% and 0.94%, respectively.

$$\text{DLE} = \frac{\text{Weight of loaded drug}}{\text{Weight of drug in feed}} \times 100\%$$

$$\text{DLC} = \frac{\text{Weight of loaded drug}}{\text{Weight of drug loaded NPs}} \times 100\%$$

Characterization of TNPs and hydrogel formation

TNP and TNP^{GEL} were characterized in terms of their size, morphology and dynamic viscosity. Figure 2 showed that TNP/DOX/ZnPC particles, mixture of equivalent mole of TNP/DOX and TNP/ZnPC, had an average diameter of 102 nm. Compared to blank TNP, there is about 20 nm increase in diameter due to the drug encapsulation. After drug encapsulation, drug-loaded TNPs were lyophilized. Drug-loaded TNP solutions were obtained by dispersion of the dried powder in PBS. As shown in Figure 3A, after 37°C heating for 5 minutes, the solution turned uniform light red and dark green after DOX and ZnPC encapsulation, respectively, whereas blank TNP solution showed milk white at a concentration of 20% (W/W). Vial inversion and rheology test (Figure S3) showed good hydrogel formation of blank TNP and all the drug-loaded groups after 37°C heating for 5 minutes. As shown in Figure S4, TNP/DOX/ZnPC GEL showed higher G′ value than its corresponding G″, which suggested a stable hydrogel formation. These drug-loaded TNPs showed stability as long as 3 months at room temperature (data not shown). In addition, no obvious morphology difference of the hydrogel was observed in SEM images before and after drug encapsulation (Figure 2). Since ZnPC suffers from aggregation in water, which reduces its photobiological activity,[30] the above results indicated that ZnPC encapsulation by designed TNP could significantly improve its aqueous solubility (with the solubility of 1.9 mg/mL) and attribute to improving its bioavailability and photobiological activity.

The release profile of DOX and ZnPC from TNP was quantitatively studied in PBS at 37°C over 35 days. Figure 3B clearly illustrated a gradual release from TNP/DOX/ZnPC^{GEL} for both DOX and ZnPC and then a plateau phase with cumulative release of about 80%. This release profile was consistent with a similar paclitaxel-encapsulated PECT hydrogel reported by Wang et al, which explained the drug release behavior that the dilution of PBS weakened the interactions between nanoparticles gradually and eventually resulted in the breakup of the drug-loaded nanoparticles.[31] The moduli analysis after drug release for 20 days (data in Figure S5) also indicated that the hydrogel showed relatively decreased G′ value and gradually collapsed with the angular frequency increase. In addition, no obvious change in modulus data was found after the laser treatment (660 nm for 90 seconds with an intensity of 100 J/cm^2, Figure S6).

Cellular uptake of TNP/DOX/ZnPC

Cellular accumulation is the first step of chemotherapeutic agents and PS to exert their tumor inhibition activity. We studied the cellular uptake of DOX and ZnPC from TNP/DOX/ZnPC using 5637 cells. The representative figures were presented in Figure 4. A significant increase in the fluorescence intensity of ZnPC was observed compared with free ZnPC after 4 hours of incubation. As the low solubility of ZnPC caused by its significant π–π interactions, the weak fluorescence of free ZnPC-treated cells indicated that free ZnPC molecules hardly entered into 5637 cells. However, after being loaded into the TNP, more ZnPC was uptaken by 5637 cells. That is the result of cellular uptake of ZnPC-loaded TNP, which has a diameter of around 100 nm and is easily to be uptaken by tumor cells. In addition, as 17.8 μg/mL of DOX solely can enter 5637 cells well, no obvious increase

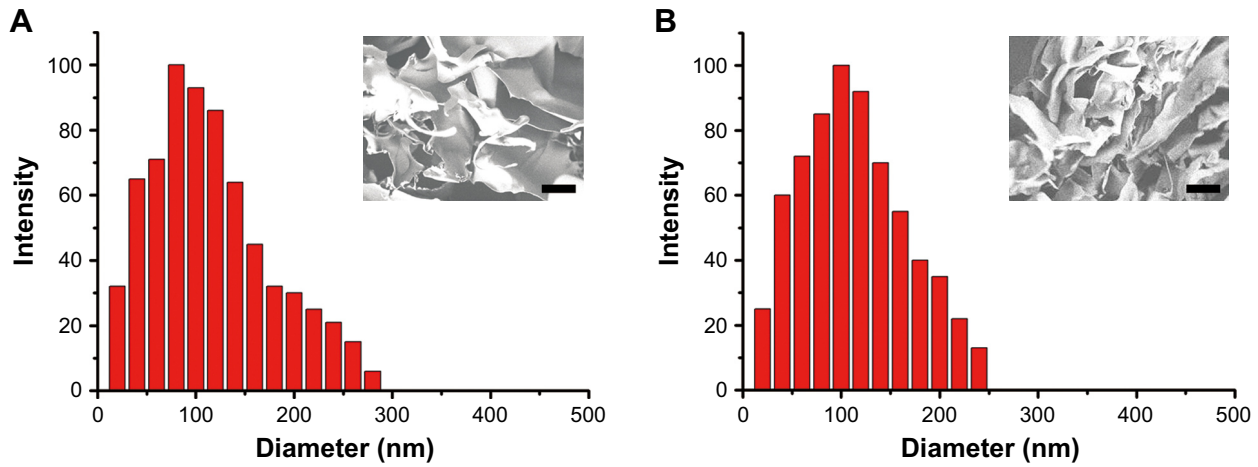

Figure 2 Particle size of (**A**) TNP and (**B**) TNP/DOX/ZnPC and SEM morphology of TNP^{GEL} (**A** inset) and TNP/DOX/ZnPC^{GEL} (**B** inset) after 37°C treatment.
Note: The scale bar was 100 nm for all the SEM images.
Abbreviations: TNP, thermal-responsive nanoparticle; TNP/DOX/ZnPC, mixture of equivalent mole of TNP/DOX and TNP/ZnPC; ZnPC, zinc phthalocyanine; SEM, scanning electron microscope.

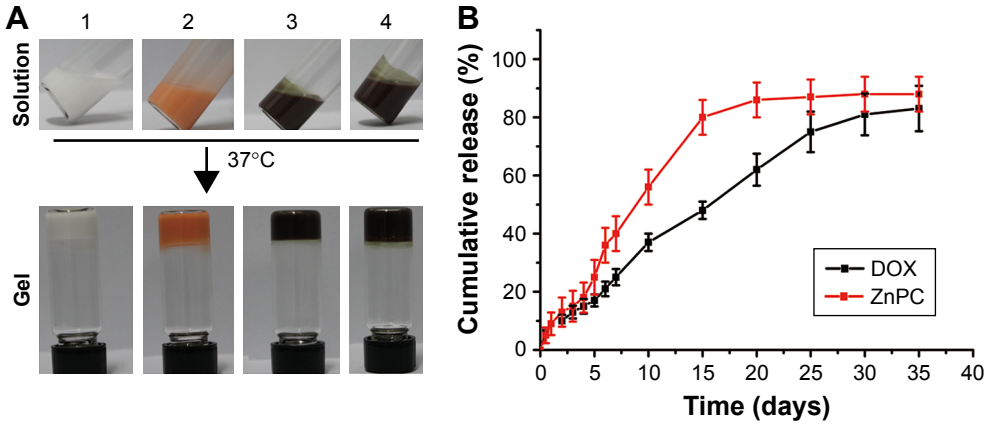

Figure 3 Optical images of blank TNP hydrogel and hydrogels after DOX and/or ZnPC encapsulation (**A**) and in vitro cumulative drug release from TNP/DOX/ZnPC hydrogel within 5 weeks with TNP/DOX:TNP/ZnPC of 1:5 (**B**). 1, 2, 3 and 4 in (**A**) means blank TNP, TNP/DOX, TNP/ ZnPC and TNP/DOX/ZnPC, specifically.
Abbreviations: DOX, doxorubicin; TNP, thermal-responsive nanoparticle; ZnPC, zinc phthalocyanine; TNP/DOX/ZnPC, mixture of equivalent mole of TNP/DOX and TNP/ZnPC.

of fluorescence intensity was found in TNP/DOX/ZnPC group. These data confirmed the enhanced cellular uptake of ZnPC by encapsulated into TNP. Further enhancement of PDT efficiency or photo/chemo combination was anticipated by TNP/DOX/ZnPC formulations.

Cell inhibition and ROS generation of TNP/DOX/ZnPC

The in vitro phototoxicity studies were performed by MTT assays on 5637 cells and exhibited in Figure 5. As there are several molecular mechanisms of DOX to kill cancer cells, such as inhibition of topoisomerase II enzyme, intercalation with DNA and production of free radicals, the rational combination of DOX and PS treatment is expected to enhance tumor elimination. Some studies have shown that combination of DOX and PDT could be more effective than their individual treatments. The findings of Kirveliene et al showed that the effect of PDT alone was significantly enhanced by the combination of DOX.[32] Being well consistent with the above study, as shown in Figure 5A, our study further demonstrated significant decrease in cellular viability of 5637 cells when DOX and ZnPC was coencapsulated into TNPs than their single encapsulation. Specifically, the best cell inhibition was found when the weight ratio of DOX and ZnPC encapsulated in the TNPs reached about 1:5 with cell viability of 18.5% vs TNP/DOX of 29.7% and TNP/ZnPC of 47.4% when the total drug concentration was 1 μg/mL. The data in Figure 5A also indicated that TNP alone (without drug encapsulation) showed cell viability over 80% even at the concentration of about 1 mg/mL.

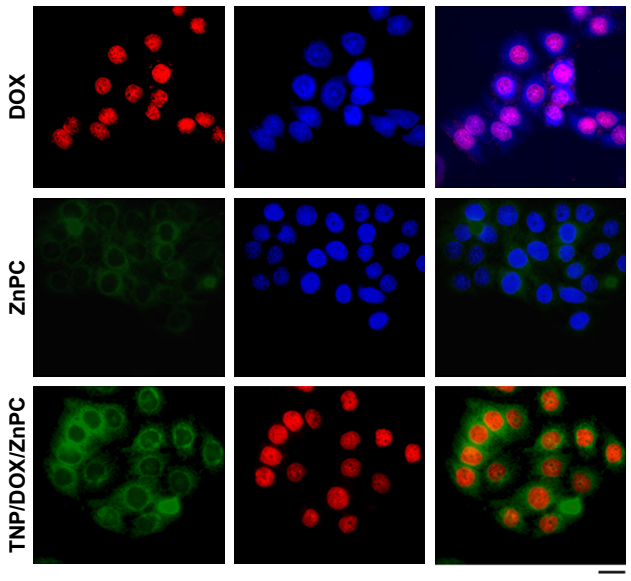

Figure 4 Cellular uptake of free drugs and TNP/DOX/ZnPC at the DOX concentration of 17.8 μg/mL and ZnPC concentration of 20 μg/mL against 5637 cells.
Note: The scale bar was 25 μm for all images.
Abbreviations: DOX, doxorubicin; TNP, thermal-responsive nanoparticle; ZnPC, zinc phthalocyanine; TNP/DOX/ZnPC, mixture of equivalent mole of TNP/DOX and TNP/ZnPC.

As ROS generation is the main mechanism of PDT, we used DCFH-DA staining to investigate the intracellular ROS generation under different formulation treatments. After 4 hours of incubation of free drug and TNP/drug formulations with or without irradiation, cellular ROS level was detected using ROS detection assay kit according to the supplier's instructions. Quantitative analysis shown in Figure 5B demonstrated that TNP/ZnPC under irradiation showed high level of ROS generation, indicating a high efficiency of TNP formulations for PDT. Specifically, TNP/ZnPC showed a 3.1-fold of ROS generation compared with free ZnPC under irradiation. This result was consistent with the work by Yu et al,[33] in which ZnPC was loaded into PEG-PMAN polymer micelles and showed significantly higher ROS generation in osteosarcoma cells. Zhao et al

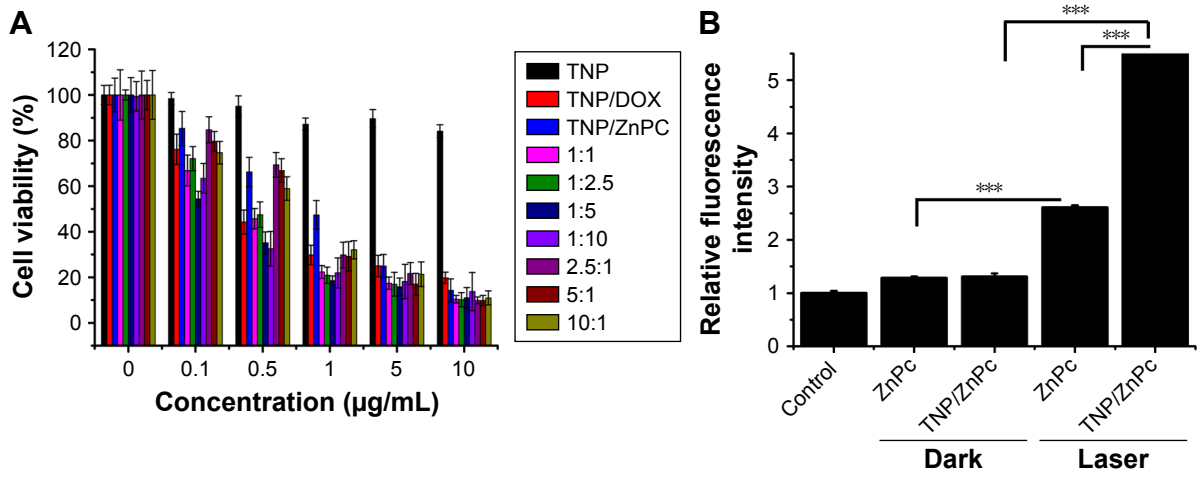

Figure 5 (**A**) In vitro cellular killing efficiency of TNP/DOX/ZnPC with laser irradiation at different weight ratios of DOX and ZnPC determined by MTT assay at 24 hours.
Notes: Concentrations of TNP were equal to the amount of TNP in corresponding drug-loaded group. (**B**) Cellular ROS generation assay of free ZnPC and TNP/DOX/ZnPC with weight ratio of DOX:ZnPC=1:5 in 5637 cells at 4 hours postincubation. Laser irradiation was 100 J/cm^2, 660 nm, 120 seconds. (n=6, ***$P<0.001$.)
Abbreviations: DOX, doxorubicin; TNP, thermal-responsive nanoparticle; ZnPC, zinc phthalocyanine; TNP/DOX/ZnPC, mixture of equivalent mole of TNP/DOX and TNP/ZnPC.

have encapsulated silicon PC using silica nanoparticles, which generated $^1O_2$ more efficiently than free control.[34] In addition, encouraged by the good cell inhibition of TNP/DOX/ZnPC with DOX/ZnPC weight ratio of 1:5, ROS generation was also analyzed at this ratio. As shown in Figure 5B, TNP/DOX/ZnPC generated relative high level of ROS with 4.8-fold of free ZnPC and 1.6-fold of TNP/ZnPC. These results was consistent with the good 5637 cells inhibition of TNP/DOX/ZnPC and further indicated that DOX could effectively enhance ROS generation of TNP/ZnPC. The study by Zakaria et al[35] supports such evidence with their recent investigation into the synergistic effect of low doses of combined Doxil® and aminoleuvic acid-based PDT on MCF-7 cells.

Inhibition of TNP/DOX/ZnPC on 5637 cells xenograft

We further studied the in vivo anti-tumor of TNP/DOX/ZnPC in 5637 cells xenograft model. The results in Figure 6 showed a better outcome of DOX and ZnPC combination therapy (TNP/DOX/ZnPC, **$P<0.01$ vs TNP/DOX and TNP/ZnPC plus laser). In detail, TNP/DOX and TNP/ZnPC showed a tumor volume of 21.0- and 22.4-fold of its original tumor volume at day 20, respectively. However, TNP/DOX/ZnPC

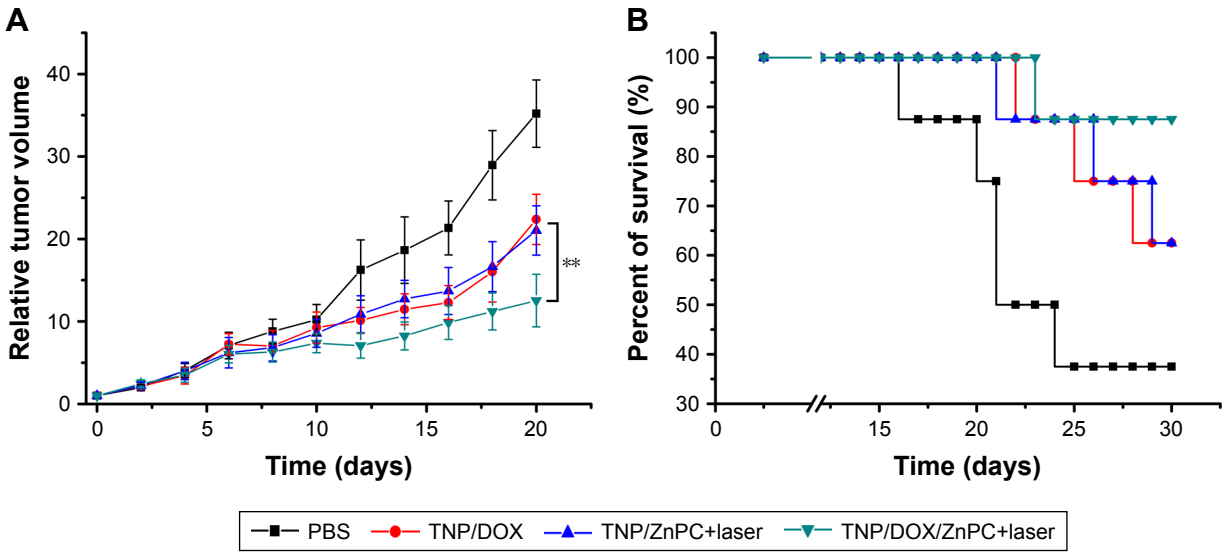

Figure 6 In vivo 5637 cells xenograft inhibition analysis.
Notes: Relative tumor volume (**A**) and survival percentage (**B**) after different treatments at day 0 with DOX and/or ZnPC was administrated at a total dose of 20 mg/kg body weight (n=6, **$P<0.01$).
Abbreviations: DOX, doxorubicin; TNP, thermal-responsive nanoparticle; ZnPC, zinc phthalocyanine.

treatment further reduced the tumor growth and showed only 12.5-fold of its original tumor volume (Figure 6A). Furthermore, TNP/DOX/ZnPC treatment generated a slightly higher survival of 87.5% (vs 62.5% of TNP/DOX or TNP/ZnPC treatment, Figure 6B) at the destination of the study. Moreover, compared with free DOX and ZnPC, TNP/DOX/ZnPC treatment also showed significantly higher tumor inhibition (Figure S7). This high tumor inhibition might mainly attribute to the high local drug concentration released by in situ gel administration. In addition, the synergistic effect of DOX and ZnPC in TNP/DOX/ZnPC on ROS generation as illustrated in Figure 5B might be helpful for this combination therapy. However, further mechanism of this enhancement, such as the influence on apoptosis and necrosis, mitochondrial function and DNA fragmentation, might be intricate and will be further studied.

Conclusion

As have extensively been reported as effective drug delivery agent, nanoscience-based system is gradually providing hope for cancer diagnosis and therapy. However, the fate of these biodegradable nanoparticles after system administration and its potential risk are currently being assessed. With enhanced specificity and improved therapeutic accuracy, in situ-formed smart hydrogels are definitely of great interest for solid tumor management such as bladder cancer and breast cancer. However, multiple drug combination placed a great hope to overcome the high failure rate of single-agent therapy or single-regimen therapy. PDT coupled with chemotherapy agent have proven to be a promising combination treatment for some kinds of tumors. On the basis of all the in vitro and in vivo tumor inhibition measurements in this contribution, it can be concluded that thermal-sensitive TNP^{GEL} are promising in situ-formed matrix for DOX- and ZnPC-based photo/chemo combination treatment for bladder cancer therapy. Furthermore, with rational design of drug encapsulation, this in situ-formed TNP^{GEL} could be explored as matrix for other local combination treatment regimens.

Disclosure

The authors report no conflicts of interest in this work.

References

1. Kamat AM, Hahn NM, Efstathiou JA, et al. Bladder cancer. *Lancet*. 2016;388(10061):2796–2810.
2. Voltaggio L, Cimino-Mathews A, Bishop JA, et al. Current concepts in the diagnosis and pathobiology of intraepithelial neoplasia: a review by organ system. *CA Cancer J Clin*. 2016;66(5):408–436.
3. Huncharek M, Geschwind JF, Witherspoon B, Mcgarry R, Adcock D. Intravesical chemotherapy prophylaxis in primary superficial bladder cancer: a meta-analysis of 3703 patients from 11 randomized trials. *J Clin Epidemiol*. 2000;53(7):676–680.
4. Dougherty TJ, Grindey GB, Fiel R, Weishaupt KR, Boyle DG. Photoradiation therapy. II. Cure of animal tumors with hematoporphyrin and light. *J Natl Cancer Inst*. 1975;55(1):115–121.
5. Rkein AM, Ozog DM. Photodynamic therapy. *Dermatol Clin*. 2014;32(3):415–425.
6. Chiaviello A, Postiglione I, Palumbo G. Targets and mechanisms of photodynamic therapy in lung cancer cells: a brief overview. *Cancers*. 2011;3(1):1014–1041.
7. Nadhman A, Nazir S, Khan MI, et al. Visible-light-responsive ZnCuO nanoparticles: benign photodynamic killers of infectious protozoans. *Int J Nanomedicine*. 2015;10:6891–6903.
8. Muehlmann LA, Ma BC, Longo JP, Almeida Santos MF, Azevedo RB. Aluminum-phthalocyanine chloride associated to poly(methyl vinyl ether-co-maleic anhydride) nanoparticles as a new third-generation photosensitizer for anticancer photodynamic therapy. *Int J Nanomedicine*. 2014;9:1199–1213.
9. Sakamoto K, Ohno-Okumura E, Keiichi Sakamoto EO-O. Syntheses and functional properties of phthalocyanines. *Materials*. 2009;2(3):1127–1179.
10. Fabris C, Soncin M, Miotto G, et al. Zn(II)-phthalocyanines as photothertherapeutic agents for cutaneous diseases. Photosensitization of fibroblasts and keratinocytes. *J Photochem Photobiol B*. 2006;83(1):48–54.
11. Mfouo-Tynga I, Abrahamse H. Cell death pathways and phthalocyanine as an efficient agent for photodynamic cancer therapy. *Int J Mol Sci*. 2015;16(5):10228–10241.
12. Dolmans DE, Fukumura D, Jain RK. Photodynamic therapy for cancer. *Nat Rev Cancer*. 2003;3(5):380–387.
13. Hadjur C, Wagnières G, Ihringer F, Monnier P, van den Bergh H. Production of the free radicals O2.- and .OH by irradiation of the photosensitizer zinc(II) phthalocyanine. *J Photochem Photobiol B*. 1997;38(2–3):196–202.
14. Love WG, Duk S, Biolo R, Jori G, Taylor PW. Liposome-mediated delivery of photosensitizers: localization of zinc (II)-phthalocyanine within implanted tumors after intravenous administration. *Photochem Photobiol*. 1996;63(5):656–661.
15. Sekkat N, van den Bergh H, Nyokong T, Lange N. Like a bolt from the blue: phthalocyanines in biomedical optics. *Molecules*. 2011;17(1):98–144.
16. Rajora MA, Lou JWH, Zheng G. Advancing porphyrin's biomedical utility via supramolecular chemistry. *Chem Soc Rev*. 2017;46(21):6433–6469.
17. Ramasamy T, Ruttala HB, Gupta B, et al. Smart chemistry-based nanosized drug delivery systems for systemic applications: a comprehensive review. *J Control Release*. 2017;258:226–253.
18. Kamkaew A, Chen F, Zhan Y, Majewski RL, Cai W. Scintillating nanoparticles as energy mediators for enhanced photodynamic therapy. *ACS Nano*. 2016;10(4):3918–3935.
19. Qian X, Zheng Y, Chen Y. Micro/Nanoparticle-augmented sonodynamic therapy (SDT): breaking the depth shallow of photoactivation. *Adv Mater*. 2016;28(37):8097–8129.
20. Taratula O, Patel M, Schumann C, et al. Phthalocyanine-loaded graphene nanoplatform for imaging-guided combinatorial phototherapy. *Int J Nanomedicine*. 2015;10:2347–2362.
21. da Volta Soares M, Oliveira MR, dos Santos EP, et al. Nanostructured delivery system for zinc phthalocyanine: preparation, characterization, and phototoxicity study against human lung adenocarcinoma A549 cells. *Int J Nanomedicine*. 2011;6:227–238.
22. Ramasamy T, Haidar ZS, Tran TH, et al. Layer-by-layer assembly of liposomal nanoparticles with PEGylated polyelectrolytes enhances systemic delivery of multiple anticancer drugs. *Acta Biomater*. 2014;10(12):5116–5127.
23. Habiba K, Encarnacion-Rosado J, Garcia-Pabon K, et al. Improving cytotoxicity against cancer cells by chemo-photodynamic combined modalities using silver-graphene quantum dots nanocomposites. *Int J Nanomedicine*. 2016;11:107–119.
24. Aniogo EC, George BPA, Abrahamse H. Phthalocyanine induced phototherapy coupled with Doxorubicin; a promising novel treatment for breast cancer. *Expert Rev Anticancer Ther*. 2017;17(8):693–702.

25. Zakaria S, Gamal-Eldeen AM, El-Daly SM, Saleh S. Synergistic apoptotic effect of Doxil® and aminolevulinic acid-based photodynamic therapy on human breast adenocarcinoma cells. *Photodiagnosis Photodyn Ther*. 2014;11(2):227–238.
26. Diez B, Ernst G, Teijo MJ, Batlle A, Hajos S, Fukuda H. Combined chemotherapy and ALA-based photodynamic therapy in leukemic murine cells. *Leuk Res*. 2012;36(9):1179–1184.
27. Conde J, Oliva N, Zhang Y, Artzi N. Local triple-combination therapy results in tumour regression and prevents recurrence in a colon cancer model. *Nat Mater*. 2016;15(10):1128–1138.
28. Huang P, Zhang Y, Wang W, et al. Co-delivery of doxorubicin and (131) I by thermosensitive micellar-hydrogel for enhanced in situ synergetic chemoradiotherapy. *J Control Release*. 2015;220(Pt A):456–464.
29. Huang P, Song H, Zhang Y, et al. FRET-enabled monitoring of the thermosensitive nanoscale assembly of polymeric micelles into macroscale hydrogel and sequential cognate micelles release. *Biomaterials*. 2017;145:81–91.
30. Ricci-Júnior E, Marchetti JM. Preparation, characterization, photocytotoxicity assay of PLGA nanoparticles containing zinc (II) phthalocyanine for photodynamic therapy use. *J Microencapsul*. 2006;23(5):523–538.
31. Wang W, Deng L, Xu S, et al. A reconstituted "two into one" thermosensitive hydrogel system assembled by drug-loaded amphiphilic copolymer nanoparticles for the local delivery of paclitaxel. *J Mater Chem B*. 2013;1:12.
32. Kirveliene V, Grazeliene G, Dabkeviciene D, et al. Schedule-dependent interaction between Doxorubicin and mTHPC-mediated photodynamic therapy in murine hepatoma in vitro and in vivo. *Cancer Chemother Pharmacol*. 2006;57(1):65–72.
33. Yu W, Ye M, Zhu J, et al. Zinc phthalocyanine encapsulated in polymer micelles as a potent photosensitizer for the photodynamic therapy of osteosarcoma. *Nanomedicine*. 2018;14(4):1099–1110.
34. Zhao B, Yin JJ, Bilski PJ, Chignell CF, Roberts JE, He YY. Enhanced photodynamic efficacy towards melanoma cells by encapsulation of Pc4 in silica nanoparticles. *Toxicol Appl Pharmacol*. 2009;241(2):163–172.
35. Zakaria S, Gamal-Eldeen AM, El-Daly SM, Saleh S. Synergistic apoptotic effect of Doxil® and aminolevulinic acid-based photodynamic therapy on human breast adenocarcinoma cells. *Photodiagnosis Photodyn Ther*. 2014;11(2):227–238.